

Trigger Strategy for the Charged Higgs Boson Search

Chris Potter (for the ATLAS Collaboration)*

McGill University

E-mail: chris.potter@cern.ch

At hadron colliders, the physics interaction rate exceeds the capacity of modern electronics to write out every event. Rare phenomena, with typical cross sections several orders of magnitude below Standard Model process cross sections, therefore require a strategy for optimal triggering. We describe the trigger strategy for the charged Higgs boson search at the ATLAS and CMS experiments at the Large Hadron Collider, with a detailed description of the ATLAS planned strategy

Prospects for Charged Higgs Discovery at Colliders

September 16-19 2008

Uppsala, Sweden

*Speaker.

1. Introduction

1.1 Models with Charged Higgs Bosons

In the Standard Model (SM) of particle physics, a single Higgs doublet performs the task of electroweak symmetry breaking. This model predicts a single neutral scalar Higgs boson. A charged Higgs boson H^\pm is predicted by theoretical models with two or more Higgs doublets. The Minimal Supersymmetric Model (MSSM) [1] assumes the two Higgs doublet model (2HDM) while the Next to Minimal Supersymmetric Model (NMSSM) [2] adds a singlet Higgs field to the 2HDM. Both predict the existence of the H^\pm .

In all models which predict the H^\pm , the production cross sections at colliders are predicted to be multiple orders of magnitude below Standard Model processes, and are therefore considered rare phenomena. For the H^\pm search, or indeed any search for rare phenomena at colliders, the need for a trigger strategy originates in a fundamental limitation of modern electronics: the maximum rate at which events can be reliably written to storage. This maximum rate is of order a few hundred Hz. If the physics interaction rate is lower than this limit, all physics events can be written out for subsequent analysis. If the physics interaction rate is higher than this limit, then a trigger strategy for optimally filtering signal events becomes necessary.

In this section we first describe trigger strategies at past and present colliders and next outline a generic trigger strategy for rare phenomena. In the following sections we focus on the trigger strategies for the H^\pm search at CMS and ATLAS, the two general purpose detectors at the Large Hadron Collider (LHC).

1.2 Charged Higgs Boson Searches at Colliders

Direct searches for the charged Higgs boson have been undertaken at LEP and the Tevatron, and indirect searches have been undertaken at the B factories Belle and Babar. At LEP, a search for $e^+e^- \rightarrow H^+H^-$ yielded the first direct limits on the H^\pm mass [3]. At Belle and BaBar, limits on the processes $B^+ \rightarrow \tau^+\nu$ and $b \rightarrow s\gamma$ [4] have probed the extent to which an H^\pm could mediate these processes.

For the e^+e^- colliders LEP, Belle and Babar, only a minimal trigger strategy is necessary since the interaction rate is near or below the upper limit on the maximum rate events can be written to storage. At Babar, for example, the total physics interaction rate for fermion pair production $e^+e^- \rightarrow \ell^+\ell^-, q\bar{q}$ was approximately 180 Hz at design luminosity, and the trigger was approximately 99% efficient for $B\bar{B}$ events [5]. Indeed, the primary purpose of the Babar trigger was to reduce the 20 kHz rate from beam-induced backgrounds rather than physics events.

At hadron colliders, however, the physics interaction rate far exceeds the upper limit on the trigger rate. At design luminosity, the LHC bunch crossing rate is expected to be 40 MHz with multiple physics interactions per bunch crossing[6]. The trigger strategy for the H^\pm search at the LHC will be discussed in the following sections. At the Tevatron, where the interaction rate also requires a careful trigger strategy for rare phenomena, searches for the light H^\pm ($m_{H^\pm} < m_{top}$) at both CDF and D0 have relied on the same trigger strategy for triggering on $t\bar{t}$ events since the decays products of the H^\pm in many models are similar to those of the W boson [7, 8].

D0 carried out the only direct search for the heavy H^\pm ($m_{H^\pm} > m_{top}$) at the Tevatron [9], and relied on the same trigger signatures as the single top search: $e+2\text{jets}$ and $\mu+\text{jet}$ [10]. The evolu-

$\int dtL$ [pb^{-1}]	Electron E_T [GeV]	Jet 1 E_T [GeV]	Jet 2 E_T [GeV]
103	15	15	15
330	15	20	20
619	15	25	20
913	15	30	30

Table 1: The evolution of the $D\emptyset e+2\text{jets}$ trigger thresholds from August 2002 to December 2005. As instantaneous luminosity rises, trigger thresholds must tighten to maintain the trigger bandwidth budget.

tion over time of the thresholds and isolation criteria for these signatures illustrates the competing imperatives to stay within the trigger bandwidth budget yet maintain maximal signal trigger efficiency. See Table 1.2 for the evolution of the trigger thresholds in the $e+2\text{jets}$ signature from August 2002 to December 2005. As the instantaneous luminosity increases, trigger signature E_T thresholds must rise and/or isolation criteria must tighten, but in a way such that the signal efficiency decreases as little as possible.

1.3 Generic Trigger Strategy for Rare Phenomena

A generic trigger strategy for rare phenomena demands the highest possible signal efficiency with respect to the offline-selected events while keeping the overall trigger rates within the acceptable upper bound. To this end, these principles are enjoined:

- use of unrescaled triggers with the lowest E_T threshold available,
- use of single object triggers if possible, otherwise optimized multiple object triggers,
- use of the most realistic overall trigger signature rate estimates possible and
- careful monitoring of trigger algorithm performance in the signal simulation.

Prescaled signatures are useless for triggering on rare phenomena since they are inefficient by design. As realistic overall trigger rates for different signatures become available, previously unrescaled signatures may become prescaled and will therefore become obsolete for triggering on rare phenomena. In that case the strategy should be to use a similar signature with a higher threshold which is still unrescaled.

Trigger signature efficiencies will need to be measured in data. Using single object triggers (as opposed to multiple objects AND-ed together) simplifies measuring trigger efficiencies from data and applying them to simulation. These efficiencies can be obtained from the trigger simulation, but the simulation may not match very well the performance of the real trigger. On the other hand, when multiple object signatures become necessary, their thresholds should be optimized for signal selection.

In a running experiment, the trigger rates are directly measured and the trigger rate must be in accord with the overall search priorities of the experiment. In developing a trigger strategy for a rare phenomenon at a future experiment, the most realistic trigger rate estimates should be used in order to legitimize its use.

Production/Decay	BR	ATLAS/CMS	Trigger Objects
$t\bar{t} \rightarrow 2bW_{lep}\tau_{lep}\nu$	0.076	No/No	j,b, e, mu, E_T^{miss}
$t\bar{t} \rightarrow 2bW_{lep}\tau_{had}\nu$	0.140	Yes/Yes	j,b, e, mu, tau, E_T^{miss}
$t\bar{t} \rightarrow 2bW_{had}\tau_{lep}\nu$	0.276	Yes/No	j,b, e,mu, E_T^{miss}
$t\bar{t} \rightarrow 2bW_{had}\tau_{had}\nu$	0.508	Yes/No	j,b, tau, E_T^{miss}
$gg \rightarrow 4bW_{lep}W_{lep}$	0.046	No/No	j,b, e,mu, E_T^{miss}
$gg \rightarrow 4bW_{lep}W_{had}$	0.338	Yes/Yes	j,b, e,mu, E_T^{miss}
$gg \rightarrow 4bW_{had}W_{had}$	0.611	No/No	j,b
$gg \rightarrow 2bW_{lep}\tau_{lep}\nu$	0.076	No/No	j,b,e,mu, E_T^{miss}
$gg \rightarrow 2bW_{lep}\tau_{had}\nu$	0.140	No/No	j,b,e,mu,tau, E_T^{miss}
$gg \rightarrow 2bW_{had}\tau_{lep}\nu$	0.276	No/No	j,b,e,mu, E_T^{miss}
$gg \rightarrow 2bW_{had}\tau_{had}\nu$	0.508	Yes/Yes	j,b,tau, E_T^{miss}

Table 2: The final states for charged Higgs boson decays for the low mass decay from $t\bar{t}$, high mass production from $gg/gb \rightarrow tbH^+$ with $H^+ \rightarrow tb$, and high mass production from $gg/gb \rightarrow tbH^+$ with $H^+ \rightarrow \tau\nu$. The column ATLAS/CMS indicates whether the given channel has been studied by these two Collaborations. Also shown are the branching ratios ($W \times W$ or $W \times \tau$) and relevant trigger objects.

It will always be necessary to monitor the performance of the trigger algorithms in the signal simulation with respect to offline reconstruction. Anomalous behavior of triggers in signal simulation should be corrected immediately. In principle, the offline reconstruction is the ideal reconstruction, and the trigger reconstruction should behave as much as possible like the offline reconstruction.

2. ATLAS and CMS Trigger Strategies for the Charged Higgs Boson Search

For both ATLAS and CMS, the MSSM was chosen as the appropriate benchmark for H^+ studies. Both ATLAS and CMS have studied decays to SUSY particles [11, 12], but these are not considered here. The dominant production mechanism at the LHC for the light H^+ in the MSSM is from top quark decay $t \rightarrow bH^+$. For the heavy H^+ , the dominant production mechanism is from $g\bar{b} \rightarrow \bar{t}H^+$ or $gg \rightarrow \bar{t}bH^+$. The MSSM favors the decays $H^+ \rightarrow t\bar{b}$ and $H^+ \rightarrow \tau^+\nu$ for the heavy charged Higgs boson and $H^+ \rightarrow \tau^+\nu$ for the light charged Higgs boson. From these production and decay modes, the following final states are possible:

$$tbH^+ \rightarrow 2b(W_{lep}orW_{had})(\tau_{lep}or\tau_{had}) \quad (2.1)$$

$$tbH^+ \rightarrow 4b(W_{lep}orW_{had})(W_{lep}orW_{had}) \quad (2.2)$$

$$t\bar{t} \rightarrow 2b(W_{lep}orW_{had})(\tau_{lep}or\tau_{had}) \quad (2.3)$$

where W_{lep} indicates $W \rightarrow \ell\nu$ ($\ell = e, \mu$), W_{had} indicates any other decay, τ_{lep} indicates $\tau \rightarrow \ell\nu\bar{\nu}$ ($\ell = e, \mu$) and τ_{had} indicates any other decay. Since the particle charge is not measured in the trigger, particle charges are omitted. See Table 2 for the branching ratios to these various final

Study	Trigger	Rate [Hz]
CMS	Electron $E_T^e > 29$ GeV	13
CMS	Muon $E_T^\mu > 19$ GeV	17
CMS	Tau $E_T^\tau > 93$ GeV AND $E_T^{miss} > 67$ GeV	NA
ATLAS	Electron $E_T^e > 22$ GeV AND $E_T^{miss} > 30$ GeV	10 ± 10
ATLAS	Muon $E_T^\mu > 20$ AND $E_T^{miss} > 30$ GeV	20 ± 15
ATLAS	Tau $E_T^\tau > 35$ GeV AND $E_T^{miss} > 50$ GeV	< 10
ATLAS	Tau $E_T^\tau > 45$ GeV AND $E_T^{miss} > 50$ GeV	< 10

Table 3: Trigger signatures for the H^+ search in the ATLAS and CMS studies. Rate estimates are scaled linearly to a luminosity of $10^{33} \text{ cm}^{-2} \text{ s}^{-1}$.

states and the triggerable objects in them. Table 2 also indicates which channels were studied by ATLAS and CMS.

In the light H^+ channel $t\bar{t} \rightarrow 2bW_{lep}\tau_{had}\nu$, both ATLAS and CMS produced recent studies [13, 14]. The lepton from the W boson decay provides a convenient trigger signature, and CMS chose single lepton triggers requiring $E_T^\mu > 19$ GeV (μ) for a trigger muon and $E_T^e > 29$ GeV (e) for a trigger electron. The trigger rates for these signatures at an instantaneous luminosity of $2 \times 10^{33} \text{ cm}^{-2} \text{ s}^{-1}$ were estimated at CMS to be 25 Hz (e) and 33 Hz (μ) with signal efficiency¹ near 50% in the mass range $140 < m_{H^+} < 170$ GeV. The ATLAS study for $t\bar{t} \rightarrow 2bW_{lep}\tau_{had}\nu$ chose single lepton triggers AND'ed together with E_T^{miss} triggers, primarily due to trigger rate estimates which suggest that at $10^{33} \text{ cm}^{-2} \text{ s}^{-1}$, single lepton trigger thresholds will be too high. The ATLAS studies use trigger $E_T^{miss} > 30$ GeV together either with trigger $E_T^e > 22$ GeV (e) or trigger $E_T^\mu > 20$ (μ). The signature rate estimates at $10^{33} \text{ cm}^{-2} \text{ s}^{-1}$ are 10 ± 10 Hz (e) and 20 ± 15 GeV (μ) respectively. The ATLAS analysis also uses a single hadronic tau trigger $E_T^\tau > 35$ GeV² AND'ed together with trigger $E_T^{miss} > 50$ GeV, and estimate the trigger rate at $10^{33} \text{ cm}^{-2} \text{ s}^{-1}$ to be below 10 Hz with signal efficiency near 50% to 60% for masses in the range $90 < m_{H^+} < 150$ GeV.

Both ATLAS and CMS studied the heavy $H^+ \rightarrow t\bar{b}$ decay with final state $4bW_{lep}W_{had}$ [13, 15]. The leptonic W boson decay again provides a convenient trigger strategy in that the final state has both a lepton and substantial E_T^{miss} . The ATLAS trigger signatures for this mode are $E_T^{miss} > 30$ GeV together either with trigger $E_T^e > 22$ GeV (e) or trigger $E_T^\mu > 20$ (μ). These signatures, which give signal efficiencies near 60% to 75% in the mass range $200 < m_{H^+} < 600$ GeV, are the same for the light H^+ search with the same rate estimates. The CMS study used the same trigger signatures as for its light H^+ search, namely single lepton triggers requiring $E_T^\mu > 19$ GeV (μ) or $E_T^e > 29$ GeV (e), which CMS reports give signal efficiencies of 16% in the muon channel only. The CMS strategy has the advantage of a simpler trigger, easier to monitor and understand with collision data. On the other hand, the additional requirement of missing transverse momentum, is expected to provide a second handle to reduce the trigger rate, which should prove useful at high luminosity.

In the event that CMS has underestimated trigger rates for these single lepton signatures, the

¹Signal efficiencies reported here are with respect to all generated events, rather than all offline-selected events. ATLAS H^+ trigger efficiencies with respect to offline-selected events range from 96% – 99%.

²Tau E_T refers to the visible E_T of the tau decay products.

ATLAS strategy of combining them with E_T^{miss} may prove worthwhile despite the complications in measuring these trigger efficiencies in data.

Finally, for the heavy $H^+ \rightarrow \tau^+ \nu$ decay with final state $2bW_{had} \tau_{had} \nu$, both ATLAS and CMS chose hadronic tau triggers AND'ed together with E_T^{miss} [13, 16]. For CMS, the signature is a hadronic tau with $E_T^\tau > 93$ GeV and $E_T^{miss} > 67$ GeV. CMS further required that the leading track in the reconstructed tau jet satisfy isolation criteria and have $E_T > 25$ GeV. CMS reports signal efficiencies of 10% to 40% for $170 < m_{H^+} < 600$ GeV. For ATLAS, the signature is a hadronic tau with $E_T^\tau > 45$ GeV and $E_T^{miss} > 50$ GeV. The ATLAS study estimates signal efficiencies of 20% to 40% in the same mass range $170 < m_{H^+} < 600$ GeV. The CMS study provides no signature rate estimates, but the ATLAS study estimates this trigger signature will take less than 10 Hz of the overall trigger budget.

Two channels were studied by ATLAS but not by CMS: the light H^+ produced in $t\bar{t}$ decays in which the W boson decays hadronically and the τ decays either leptonically or hadronically. Both of these analyses [13] used trigger signatures already discussed, namely $E_T^\tau > 30$ GeV and $E_T^{miss} > 50$ GeV for the hadronic tau channel and $E_T^{miss} > 30$ GeV together either with trigger $E_T^e > 22$ GeV (e) or trigger $E_T^\mu > 20$ (μ) for the leptonic τ channel. See Table 3 for a summary of the triggers used by CMS and ATLAS for the channels considered in this section. It should be noted that neither ATLAS nor CMS investigated the use of a b -tag trigger for H^+ searches. While these triggers may take time to commission, they may prove to be of some value in particular to the $H^+ \rightarrow t\bar{b}$ search in which both W bosons decay hadronically.

3. ATLAS Trigger Study for the Charged Higgs Boson Search

3.1 Signal Study Sample

In this section we study the motivation for the ATLAS trigger strategy described in the previous section. For this study, simulation samples were generated for the high mass $gg \rightarrow 4bW_{lep}W_{had}$, the high mass $gg \rightarrow 2bW_{had} \tau_{had} \nu$, the low mass $t\bar{t} \rightarrow 2bW_{lep} \tau_{had} \nu$, the low mass $t\bar{t} \rightarrow 2bW_{had} \tau_{lep} \nu$ and the low mass $t\bar{t} \rightarrow 2bW_{lep} \tau_{had} \nu$. These will be designated as follows:

- Sample A: $gg \rightarrow tbH_{400}^+ \rightarrow 2bW_{had} \tau_{had} \nu$ ($m_{H^+} = 400$ GeV).
- Sample B: $gg \rightarrow tbH_{250}^+ \rightarrow 4bW_{lep}W_{had}$ ($m_{H^+} = 250$ GeV).
- Sample C: $t\bar{t} \rightarrow \bar{t}bH_{130}^+ \rightarrow 2bW_{had} \tau_{had} \nu$ ($m_{H^+} = 130$ GeV).
- Sample D: $t\bar{t} \rightarrow \bar{t}bH_{130}^+ \rightarrow 2bW_{had} \tau_{lep} \nu$ ($m_{H^+} = 130$ GeV).
- Sample E: $t\bar{t} \rightarrow \bar{t}bH_{90}^+ \rightarrow 2bW_{lep} \tau_{had} \nu$ ($m_{H^+} = 90$ GeV).

Note that each sample represents a broader class of samples where major differences in decays and kinematic distributions are not expected.

3.2 Trigger Objects

While the trigger aims to mimic the offline reconstruction as closely as possible, divergences are inevitable. The efficiency of the trigger to reconstruct objects found in the offline reconstruction with similar properties $(\eta, \phi, E_T)^3$ gives an indication of how much divergence obtains. The E_T resolution of trigger objects indicates the ability of the trigger to reconstruct an offline object with similar E_T . The efficiency must be high in all (η, ϕ) regions of the detector and for as broad a range of E_T as possible, and the E_T resolution must be as small as possible.

Samples A, C and E represent the class of channels which contain a hadronic tau and therefore trigger taus are studied for these channels. Samples B, D and E represent the class of channels which contain a single high E_T electron or muon and therefore trigger electrons and muons are studied for these channels. E_T^{miss} is important for triggering in most of these channels, so this is also studied.

In the searches for $H^+ \rightarrow \tau_{had} \nu$, the hadronic tau trigger must perform well with respect to the offline reconstruction. The tau trigger objects for the tau signatures must be reconstructed with high efficiency. The trigger E_T^{miss} must closely match the offline E_T^{miss} for these channels. Similarly, the searches for $H^+ \rightarrow \tau_{lep} \nu$ and $H^+ \rightarrow tb \rightarrow 2bW_{lep}$ will require high efficiency of the trigger electrons and muons with respect to the offline-reconstructed electrons and muons. For higher luminosities the lepton signatures will be required in combination with E_T^{miss} , so the performance of the trigger E_T^{miss} must be monitored closely.

The measured E_T of trigger electrons, muons, hadronic taus, jets and E_T^{miss} must closely match their counterparts in the offline reconstruction and therefore their resolution must be small. The E_T threshold for all of these trigger objects is imposed by the trigger, so any divergence between the E_T measured in the trigger and the E_T measured in the offline reconstruction should be noted and corrected.

A trigger object is considered *matched* to a corresponding offline object if $\Delta R \equiv \sqrt{\Delta\eta^2 + \Delta\phi^2} < \Delta^{max}R$, where $\Delta^{max}R$ is a fixed parameter. The following definitions for efficiency (ϵ), purity (p) and resolution (r) are used:

$$\epsilon \equiv N_{trigger}^{match} / N_{offline} \quad (3.1)$$

$$p \equiv N_{trigger}^{match} / N_{trigger} \quad (3.2)$$

$$r \equiv (E_T^{trigger} - E_T^{offline}) / E_T^{offline} \quad (3.3)$$

Note that the parameter r is only defined for matched trigger objects. The resolution is then the RMS of the distribution of r , and the offset is the mean of the distribution of r . The efficiency curves can then be fit to predefined functions to extract meaningful parameters. For example, the E_T efficiency curves are fit to the function:

$$f(E_T) = \frac{1}{2}p0 \times \left(1 + \frac{erf(E_T - p1)}{\sqrt{2}p2} \right) \quad (3.4)$$

Then the plateau efficiency is the p0 parameter in fit. A plateau purity is defined similarly.

³ η is the pseudorapidity and ϕ measures the azimuthal angle.

Trigger Object	$\Delta^{max}R$	Plateau Efficiency	Plateau Purity	E_T Resolution	E_T Offset
Sample A Tau	0.1	0.93	0.19	0.06	-0.02
Sample B Muon	0.02	0.81	0.94	0.03	-0.001
Sample C Tau	0.1	0.93	0.29	0.07	-0.03
Sample D Muon	0.02	0.78	0.97	0.02	-0.001
Sample E Electron	0.02	0.99	0.22	0.01	-0.02
Sample A E_T^{miss}	0.4	0.99	0.98	0.12	-0.21
Sample B E_T^{miss}	0.4	0.99	0.81	0.28	-0.16
Sample C E_T^{miss}	0.4	0.97	0.98	0.18	-0.21
Sample D E_T^{miss}	0.4	0.98	0.97	0.20	-0.19
Sample E E_T^{miss}	0.4	0.64	0.67	0.21	-0.16

Table 4: The performance of the trigger trigger electrons, muons, taus, jets and E_T^{miss} in the signal simulation samples where they are important. The $\Delta^{max}R$ parameter is chosen to be close to the object (η, ϕ) resolution.

For an example of trigger object efficiencies plotted against η , ϕ and E_T , as well as trigger object resolution, see Figures 2 and 1. Ideally the efficiency plotted against ϕ should be high and uniform, against η should be high and uniform, and against E_T should closely approximate a step-function as closely. The E_T resolution should be small as and the E_T offset should be near zero. If the trigger underestimates the E_T consistently, then this reduces the number of events which pass the E_T threshold and therefore decreases the signal trigger efficiency.

The plateau efficiencies, plateau purities, E_T resolution and E_T offset for the important trigger objects as measured in each signal simulation sample are reported in Table 4. The plateau efficiencies are in general high, though tau efficiencies show a decrease in efficiency above 200 GeV. The plateau purities are not critical to the trigger strategy, but they do indicate how easily the trigger object is easily faked by background processes and may therefore lead to high trigger rates. For the electrons and hadronic taus, the purities around 20%. The E_T offsets indicate that all trigger objects underestimate the offline objects, with E_T^{miss} underestimated by as much as 20%. Similarly, the E_T^{miss} resolution is as large as 20%, suggesting that improvement is necessary in the E_T^{miss} trigger. Nonetheless, the trigger objects correspond fairly well with the matched offline objects.

3.3 Trigger Signatures

Given that the ATLAS trigger objects are reconstructed well with respect to the offline reconstruction, we seek trigger signatures which combine these single objects together and specify thresholds for each. Using the generic strategy outlined in Section 1.3, we seek the single object triggers with lowest thresholds which are unrescaled. The overall trigger rate for signatures must also be kept within a trigger bandwidth budget.

The analyses of samples A, C and E will depend on hadronic tau and missing E_T . Since the unrescaled single tau and E_T^{miss} signatures have thresholds which are simply too high to retain even a modest signal efficiency, these modes will require double object triggers. High efficiency can be maintained by combining tau and E_T^{miss} signatures. The analyses of samples B and D (also E) can reliably depend on electron and muon signatures at lower luminosities. At higher luminosities,

Signal	$E_T^e > 25 \text{ GeV}$	$E_T^\mu > 20 \text{ GeV}$	$E_T^\tau > 35 \text{ GeV}$	$E_T^\tau > 35 \text{ GeV}$
	AND $E_T^{miss} > 30 \text{ GeV}$	AND $E_T^{miss} > 30 \text{ GeV}$	AND $E_T^{miss} > 50 \text{ GeV}$	AND $E_T^{miss} > 40 \text{ GeV}$
Sample A	0.01	0.03	0.36	0.35
Sample B	0.17	0.25	0.07	0.10
Sample C	0.01	0.02	0.11	0.14
Sample D	0.09	0.14	0.06	0.07
Sample E	0.21	0.24	0.23	0.24
Rate [Hz]	10 ± 10	20 ± 15	< 10	< 10

Table 5: Estimated trigger signature efficiencies and rates at an instantaneous luminosity of $10^{33} \text{ cm}^{-2} \text{ s}^{-1}$ for signal samples.

these single object triggers may have thresholds which are too high for these signal modes, and consequently double object triggers will have to be employed. Combining electron and muon signatures together with E_T^{miss} can give high signal efficiency with low overall trigger rates at a luminosity of $10^{33} \text{ cm}^{-2} \text{ s}^{-1}$, and therefore these signatures are chosen. See Table 5 for the chosen thresholds and rates at $10^{33} \text{ cm}^{-2} \text{ s}^{-1}$. The rates were calculated with seven million minimum bias events.

4. Conclusion

We have given reasons for a dedicated trigger strategy for the charged Higgs boson search at the LHC and reviewed the current strategies at CMS and ATLAS. Broadly, the strategies are similar. The strategies for the heavy $H^+ \rightarrow \tau_{had}^+ \nu$ channel in particular were similar, looking for a hadronic tau jet in conjunction with large E_T^{miss} . Only the thresholds were different, with correspondingly slightly different signal efficiencies. The differences in strategy came in the strategies for searches with leptons $\ell = e, \mu$. CMS chose single lepton trigger with fairly low thresholds on the basis of trigger rate estimates which suggest the signatures are viable at high LHC luminosities. ATLAS chose single lepton triggers in conjunction with E_T^{miss} trigger based on single lepton trigger rate estimates which would exceed a reasonable bandwidth budget at a luminosity of $10^{33} \text{ cm}^{-2} \text{ s}^{-1}$ and higher. These double object signatures will prove difficult to measure in data, but they have the benefit of higher signal efficiency and lower trigger rate.

Finally, we have demonstrated that ATLAS trigger software reconstructs trigger objects in the signal simulation with sufficient similarity to the corresponding offline reconstructed objects. This is confirmed by the high signal efficiencies in signal simulation samples both before and after offline selection. Monitoring of the trigger algorithms in signal simulation will continue to be necessary. Moreover, when the LHC turns on trigger signature rates and thresholds will need to be monitored closely as the instantaneous luminosity increases. It should be noted that both for ATLAS and CMS, the results reported here were obtained with particular software releases, which have evolved and are evolving.

References

- [1] J. F. Gunion, H. E. Haber, G. L. Kane and S. Dawson, “The Higgs Hunter’s Guide,” *Frontiers in Physics* (Addison-Wesley, Redwood City, CA, 1990).
- [2] J. R. Ellis, J. F. Gunion, H. E. Haber, L. Roszkowski and F. Zwirner, *Phys. Rev. D* **39**, 844 (1989).
- [3] G. Gomez-Ceballos [DELPHI Collaboration], *Int. J. Mod. Phys. A* **16S1B**, 839 (2001).
- [4] S. Robertson, this volume.
- [5] D. Payne [BABAR Collaboration], *Nucl. Phys. Proc. Suppl.* **121**, 235 (2003) [arXiv:hep-ex/0309035].
- [6] P. Jenni, M. Nessi, M. Nordberg and K. Smith, CERN-LHCC-2003-022 (2003)
- [7] V. M. Abazov *et al.* [D0 Collaboration], *Phys. Rev. Lett.* **88**, 151803 (2002) [arXiv:hep-ex/0102039].
- [8] A. Abulencia *et al.* [CDF Collaboration], *Phys. Rev. Lett.* **96**, 042003 (2006) [arXiv:hep-ex/0510065].
- [9] V. M. Abazov *et al.* [D0 Collaboration], arXiv:0807.0859 [hep-ex].
- [10] V. M. Abazov *et al.* [D0 Collaboration], *Phys. Rev. D* **78**, 012005 (2008) [arXiv:0803.0739 [hep-ex]].
- [11] C. Hansen, N. Gollub, K. Assamagan and T. Ekelof, *Eur. Phys. J. C* **44S2**, 1 (2005)
- [12] M. Bisset, F. Moortgat and S. Moretti, *Eur. Phys. J. C* **30**, 419 (2003) [arXiv:hep-ph/0303093].
- [13] [ATLAS Collaboration], CERN-OPEN-2008-020 (to appear)
- [14] M. Baarmand, M. Hashemi and A. Nikitenko, CERN-CMS-NOTE-2006-056 (2006)
- [15] S. Lowette, J. D’Hondt and P. Vanlaer, CERN-CMS-NOTE-2006-109 (2006)
- [16] R. Kinnunen, CERN-CMS-NOTE-2006-100 (2006)

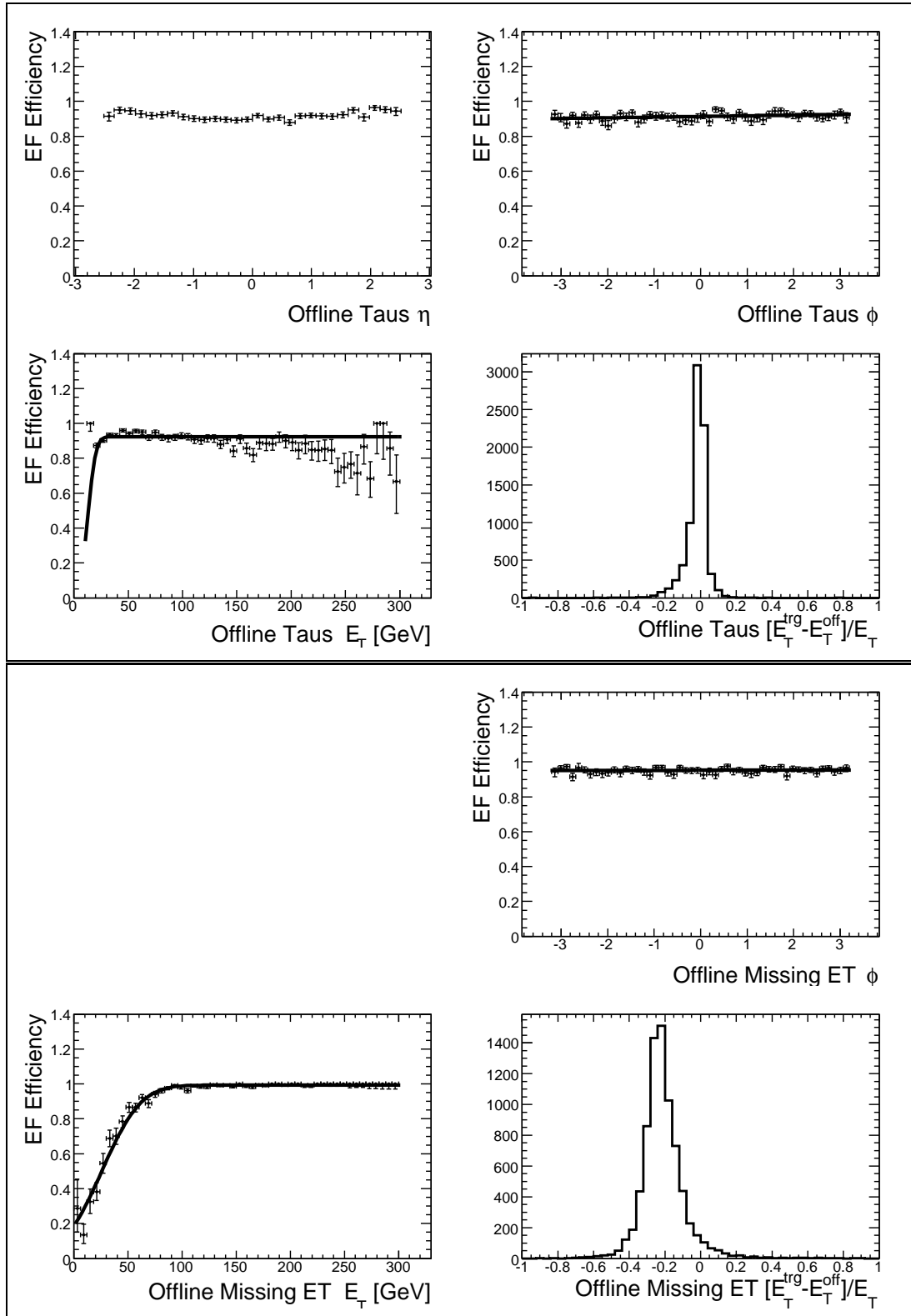


Figure 1: Sample A trigger τ (top) and trigger E_T^{miss} (bottom) efficiencies with respect to the corresponding offline object versus η , ϕ , and E_T . Resolution is also plotted.

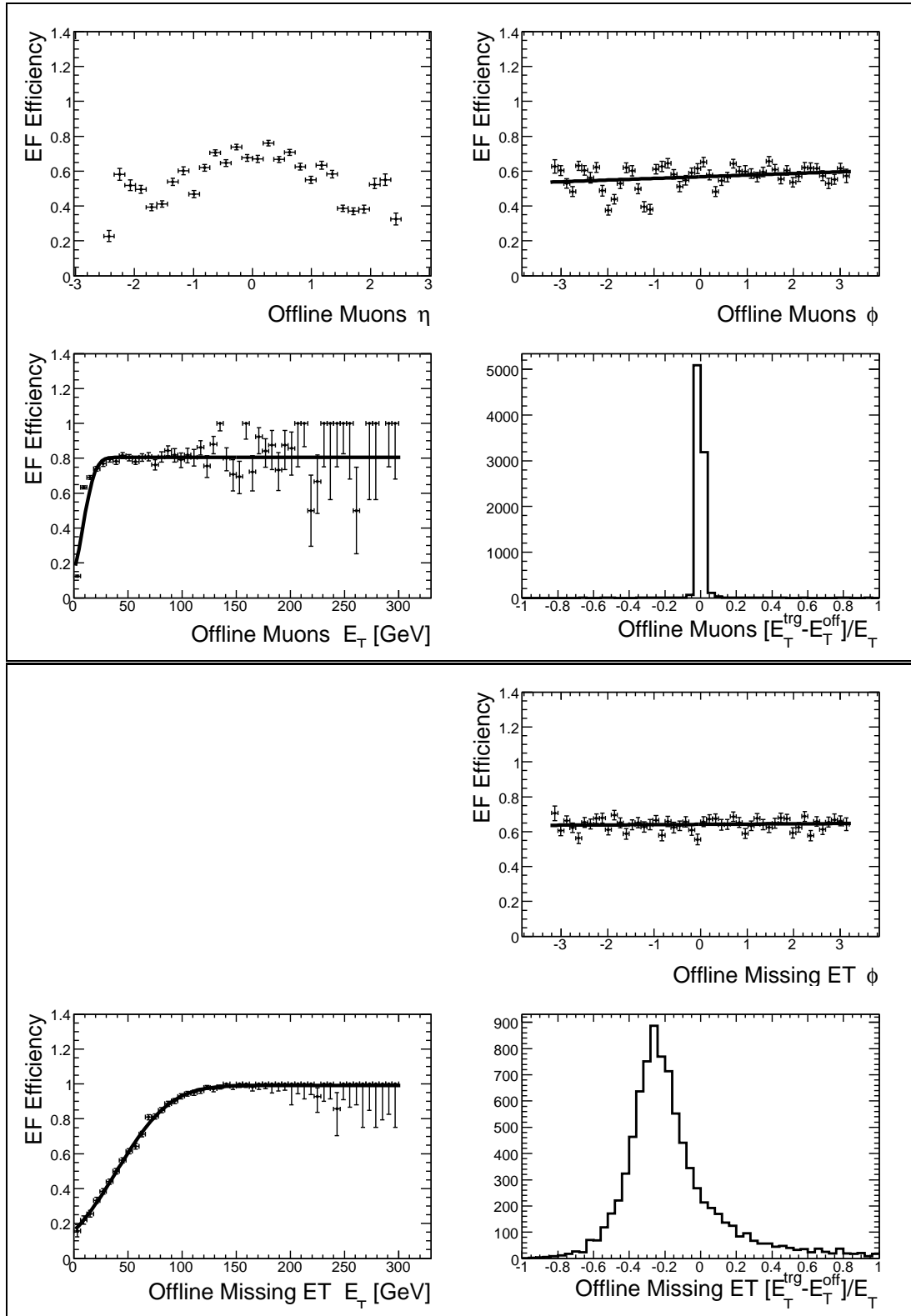


Figure 2: Sample B trigger μ (top) and trigger E_T^{miss} (bottom) efficiencies with respect to the corresponding offline object versus η , ϕ , and E_T . Resolution is also plotted.